Biochimica et Biophysica Acta 1848 (2015) 369–377

Contents lists available at ScienceDirect

Biochimica et Biophysica Acta

journal homepage: www.elsevier.com/locate/bbamem

Identification of lipid and saccharide constituents of whole microalgal cells by ^{13}C solid-state NMR ☆

Alexandre A. Arnold [a], Bertrand Genard [a], Francesca Zito [b], Réjean Tremblay [c], Dror E. Warschawski [b], Isabelle Marcotte [a,*]

[a] Department of Chemistry, Université du Québec à Montréal, and Ressources Aquatiques Québec, P.O. Box 8888, Downtown Station, Montréal H3C 3P8, Canada
[b] Laboratoire de Biologie Physico-Chimique des Protéines Membranaires, CNRS, Université Paris Diderot and Institut de Biologie Physico-Chimique, 13 rue Pierre et Marie-Curie, 75005 Paris, France
[c] Institut des Sciences de la Mer, Université du Québec à Rimouski, and Ressources Aquatiques Québec, 310 Allée des Ursulines, Rimouski, Québec G5L 3A1, Canada

ARTICLE INFO

Article history:
Received 17 April 2014
Received in revised form 2 July 2014
Accepted 15 July 2014
Available online 24 July 2014

Keywords:
Phytoplankton
Dynamic filter
Cell surface
Membrane
Organelle
Storage

ABSTRACT

Microalgae are unicellular organisms in which plasma membrane is protected by a complex cell wall. The chemical nature of this barrier is important not only for taxonomic identification, but also for interactions with exogenous molecules such as contaminants. In this work, we have studied freshwater (*Chlamydomonas reinhardtii*) and marine (*Pavlova lutheri* and *Nannochloropsis oculata*) microalgae with different cell wall characteristics. *C. reinhardtii* is covered by a network of fibrils and glycoproteins, while *P. lutheri* is protected by small cellulose scales, and the picoplankton *N. oculata* by a rigid cellulose wall. The objective of this work was to determine to what extent the different components of these microorganisms (proteins, carbohydrates, lipids) can be distinguished by ^{13}C solid-state NMR with an emphasis on isolating the signature of their cell walls and membrane lipid constituents. By using NMR experiments which select rigid or mobile zones, as well as ^{13}C-enriched microalgal cells, we improved the spectral resolution and simplified the highly crowded spectra. Interspecies differences in cell wall constituents, storage sugars and membrane lipid compositions were thus evidenced. Carbohydrates from the cell walls could be distinguished from those incorporated into sugar reserves or glycolipids. Lipids from the plasmalemma and organelle membranes and from storage vacuoles could also be identified. This work establishes a basis for a complete characterization of phytoplankton cells by solid-state NMR.
This article is part of a Special Issue entitled: NMR Spectroscopy for Atomistic Views of Biomembranes and Cell Surfaces. Guest Editors: Lynette Cegelski and David P. Weliky.

1. Introduction

Microalgae are unicellular microorganisms whose diameter typically varies between 2 and 30 μm. About 30,000 species have been identified so far in fresh and saline water, and also in harsh environments where some are adapted to extreme salinity or temperatures [1]. As for all eukaryotes, microalgae are protected by a lipid-rich plasma membrane and, in most species, a cell wall with complex composition. Cellulose, proteins, glycoproteins and polysaccharides are the most common constituents, but some microalgae are protected by a rigid wall such as the silica frustule of diatoms, or calcium carbonate for Coccolithophores. Polymers that remain undescribed are present in the microalgal cell walls which, thus, need to be further explored [2]. The chemical nature of the cell wall is an important criterion for taxonomic differentiation. It is also a critical factor when choosing species for biotechnological applications. For instance, the intracellular triglyceride reserves are coveted for biofuel production, thus cell walls must be easily broken [2].

Microalgae are at the base of the aquatic food chain; therefore the action of contaminants from human activities can impact all the trophic food web. Pollutants can bio-accumulate inside or outside the cell, and cross the microalgal cell wall to exert an adverse effect on internal sites with consequences on cell survival. It is thus important to provide tools to study their interactions and effects on the microalgal cell barrier. Because microalgae synthesize proteins, pigments and fats, particularly polyunsaturated fatty acids (PUFAs) essential for the life of higher organisms, the nutritional and energetic values of these

Abbreviations: 1D, one-dimensional; Cell, cellulose; Chry, chrysolaminarin; CP, cross polarization; DGCC, diacylglyceryl carboxyhydroxymethyl choline; DGDG, digalactosyldiglyceride; DGGA, diacylglyceryl glucuronide; DGTA, diacylglyceryl hydroxymethyl-N,N,N-trimethyl-β-alanine; DGTS, diacylglyceryl trimethylhomoserine; DHA, docosahexaenoic acid (C22:6n-3); DP, direct polarization; EPA, eicosapentaenoic acid (C20:5n-3); FA, fatty acid; Galac, galactosyl; Glyc, glycerol; HCell, hemicellulose; Hyp-O, hydroxyproline; MAS, magic-angle spinning; MGDG, monogalactosyldiglyceride; O-Gly, glycans; PC, phosphatidylcholine; PG, phosphatidylglycerol; PE, phosphatidylethanolamine; PI, phosphatidylinositol; PUFA, polyunsaturated fatty acid; SS-NMR, solid-state nuclear magnetic resonance; RINEPT, refocused-insensitive nuclei enhanced by polarization transfer; RF, radiofrequency; SQDG, (sulfoquinovosyl-diacylglycerol); TAG, triacyglyceride

☆ This article is part of a Special Issue entitled: NMR Spectroscopy for Atomistic Views of Biomembranes and Cell Surfaces. Guest Editors: Lynette Cegelski and David P. Weliky.

* Corresponding author at: Department of Chemistry, Université du Québec à Montréal, P.O. Box 8888, Downtown Station, Montréal (Qc) H3C 3P8 Canada. Tel.: +1 514 987 3000 #5015; fax: +1 514 987 4054.
E-mail address: marcotte.isabelle@uqam.ca (I. Marcotte).

http://dx.doi.org/10.1016/j.bbamem.2014.07.017
0005-2736/

constituents are being exploited in biotechnology and animal production. They are used or targeted for different applications such as biodiesel production, aquaculture feedstock, cosmetics and nutritional supplements [3]. More specifically in the prospect of energetic alternative, cultivation parameters such as light, temperature, salinity, carbon and nitrogen sources are controlled to optimize the lipids' biosynthesis [4]. Such biotechnological applications emphasize the need to provide tools to study the effects on the membrane composition of microalgae.

Ideally, the study of microalgal cell walls should not require tedious component extraction and respect cellular integrity [5]. Therefore the objective of our work is to provide a method to gain information – at a molecular level – on the cell wall components of intact microalgae. We have thus based our methodology on ^{13}C solid-state nuclear magnetic resonance (SS-NMR) since it allows screening all organic constituents. To do so, we have ^{13}C-enriched microalgae using isopically-labeled sodium bicarbonate, $NaH^{13}CO_3$. We have compared freshwater (*Chlamydomonas reinhardtii*) and marine (*Pavlova lutheri* and *Nannochloropsis oculata*) species with different cell wall characteristics and lipid profile, as detailed in Table 1. So far, ^{13}C solution NMR on intact cells has been used to study the intracellular metabolites of *Dunaliella salina* and the vacuolar triglycerides of *Neochloris oleoabundans* [6,7], while ^{1}H and ^{13}C SS-NMR with magic-angle spinning (MAS) on whole cells have provided insight on the cell wall composition of diatoms [8,9] as well as other microorganisms such as *Escherichia coli* [10–12], *Subtilis enterica* [13], *Bacillus subtilis* [14] and *Chlorobaculum tepidum* organelles [15]. To sort specific constituents according to their dynamics, we have used experiments based on through-space (cross polarization, CP) or through-bond (refocused-insensitive nuclei enhanced by polarization transfer, RINEPT) magnetization transfer to study rigid and dynamic components, respectively, as well as MAS for maximum resolution [16]. Focus was made on carbohydrate and lipid constituents. Our ^{13}C SS-NMR study of four different microalgae species highlights differences in the cell wall composition, but also in other cell components.

2. Materials and methods

2.1. Materials

N. oculata (strain: CCMP525) and *P. lutheri* (strain: CCMP1325) were obtained from the National Center for Marine Algae and Microbiota (NCMA), Bigelow Laboratory for Ocean Sciences (East Boothbay Harbor, ME, USA). The wild-type *C. reinhardtii* as well as the wall-deprived CW15 strain were obtained from the collection of the Institut de Biologie Physico-Chimique (Paris, France).

2.2. Production of ^{13}C-labeled microalgae

Microalgae were batch-cultured at 20 °C for 10 days under continuous illumination to exponential phase (4×10^6 cell/mL) in f/2 seawater medium [30] for *N. oculata* and *P. lutheri*, and TAP-medium [31] for *C. reinhardtii* (WT and CW15). Culture medium were supplemented with 1 mM sodium [^{13}C] bicarbonate ($NaH^{13}CO_3$, 99%) (Cambridge Isotope Laboratories, MA, USA) then transferred into 2.8 L polyethylene Erlenmeyer (Nalgene, Thermo Scientific, US). The culture system was sealed after addition of labeled sodium bicarbonate and the medium was purged with nitrogen gas to eliminate atmospheric CO_2. A total yield of 200–250 mg/L (dry weight) was obtained for each strain. Cells were rinsed three times with Nanopure water to eliminate traces of $NaH^{13}CO_3$ then packed by mild centrifugation into the NMR rotor (<3000 rpm).

2.3. Nuclear magnetic resonance

All spectra were recorded on a Varian Inova Unity 600 spectrometer (Agilent, Santa Clara, USA) operating at a frequency of 150.87 MHz for ^{13}C and 599.95 MHz for ^{1}H using a 4 mm double-resonance MAS probe. One-dimensional (1D) spectra were recorded with a spinning frequency of 5 kHz and a temperature maintained at 18 °C. Radiofrequency (RF) fields were 83.3 kHz for both ^{13}C and ^{1}H channels (sharp pulses, CP and decoupling). A 2 ms contact time with a 10% ramp on the ^{13}C channel was used for CP and 1 ms delays were used in the RINEPT spectra. All 1D spectra were recorded with 5 s recycle delays, 20 ms acquisition time and 2048 scans were added. A 25 Hz exponential line broadening was applied before Fourier transform. The hydration level was controlled by measuring ^{1}H spectra before and after each experiment. Spectra were processed using MNova software (Mestrelab Research, Santiago de Compostela, Spain) and referenced by setting the characteristic terminal CH_3 fatty acid (FA) peak at 14.17 ppm [9].

3. Results and discussion

The goal of this work is to ascertain the use of ^{13}C SS-NMR in the study of whole phytoplankton cells. Since the extraction of different constituents is not necessary, the localization of pathogenic species such as nanoparticles in the cell wall, plasma membrane or cytoplasm should in principle be possible. The focus is thus made on which constituents can be isolated, and whether they are present in a specific environment (cell wall, membrane). For this purpose, ^{13}C labeling is necessary in order to minimize the duration of 1D experiments – and therefore cell degradation – and to detect minor constituents. Microalgae were thus grown under autotrophic conditions in a $NaH^{13}CO_3$ environment and the resulting ^{13}C enrichment is estimated to 90% by mass spectrometry (data not shown). The study of three species – with different cell walls, types and proportions of lipids, carbohydrates, proteins and pigments – enables a better assignment of the resonances. It also allows verifying the general applicability of the NMR strategy. In addition, the identification of hydrocarbon peaks is facilitated by the comparison of the wild-type (WT) and cell-wall depleted (CW15) strains of *C. reinhardtii*.

^{13}C is a rare and not very sensitive spin, and NMR has come up with various ways to detect it, especially using magnetization transfer from the more sensitive ^{1}H spins. The most common transfer method used in SS-NMR is CP that uses strong dipolar couplings between ^{1}H and

Table 1
Characteristics of the microalgae studied.

Species (phylum, class)	Environment	Cell wall	Membrane lipids	Storage sugar
Chlamydomonas reinhardtii (Chlorophyta, Chlorophyceae)	Freshwater	Glycoproteins. No polysaccharides. Glycoproteins and oligosaccharides [16]	MGDG, DGDG, SQDG, PG, PE, DGTS [17–21]	Starch [16]
Chlamydomonas reinhardtii CW15	Freshwater	Remnants of cell walls [17]		
Pavlova lutheri (Haptophyta, Pavlovophycea)	Marine	Cellulose, hemicellulose [16]	MGDG, SQDG, DGDG, PG, DGGA, DGTA, DGCC [18,22–24]	Chrysolaminarin [16]
Nannochloropsis oculata (Heterokonphyta, Eustigmatophycaea)	Marine	Cellulose [16]	PC, MGDG, DGDG [25–27]	Chrysolaminarin [28]

^{13}C nuclei in rigid molecules. Dipolar couplings depend on motion and, in mobile molecules or mobile parts of macromolecules, are sometimes averaged out to small values, rendering CP inefficient. When this was noticed in lipids, alternative methods were borrowed from solution NMR, namely RINEPT [32–34] which exploits scalar (or *J*-) couplings between ^{1}H and ^{13}C nuclei. Scalar couplings are insensitive to motion, but scalar transfer can only occur in the transverse plane where relaxation also depends on motion. Rigid molecules quickly relax in the transverse plane and are, therefore, filtered out from RINEPT spectra. In summary, CP is efficient for rigid molecules, RINEPT for mobile molecules, and both can be used to either identify the dynamics of an observed molecule, or to filter out part of it [16]. Since ^{1}H–^{13}C transfers depend on many parameters, the most quantitative ^{13}C spectrum is obtained by direct polarization (DP), even though new sensitive methods have been recently suggested [35,36].

Fig. 1 shows the ^{13}C SS-NMR spectra acquired without dynamic filter, i.e., using direct polarization for the four microalgae studied in this work. In all cases (although with varying relative intensities) resonances are detected in regions corresponding to FAs and protein aliphatic side chains (0-40 ppm), protein C_α (40–60 ppm), C – O in carbohydrates (60–80 ppm), double bonded carbons (125–135 ppm), and amide and carbonyl regions (160–180 ppm). In addition, resonances corresponding to the C_ζ of arginine (158 ppm), and C1 anomeric carbons in glucides (ca. 100 ppm) are detected. Carbohydrate resonances fall in the following ranges: 90–112 ppm for the anomeric carbon (C1), 70–80 ppm for the ring carbons (C2-5) and 60–70 ppm for the C6 carbon. While peaks are readily observed in these regions, the resolution is poor and an overlap is expected with glycerol carbons from lipids. Similarly, resonances from the C_α and side chains of the proteins' amino acid residues should ideally be separated from the intense FA signals in the 10–50 ppm range.

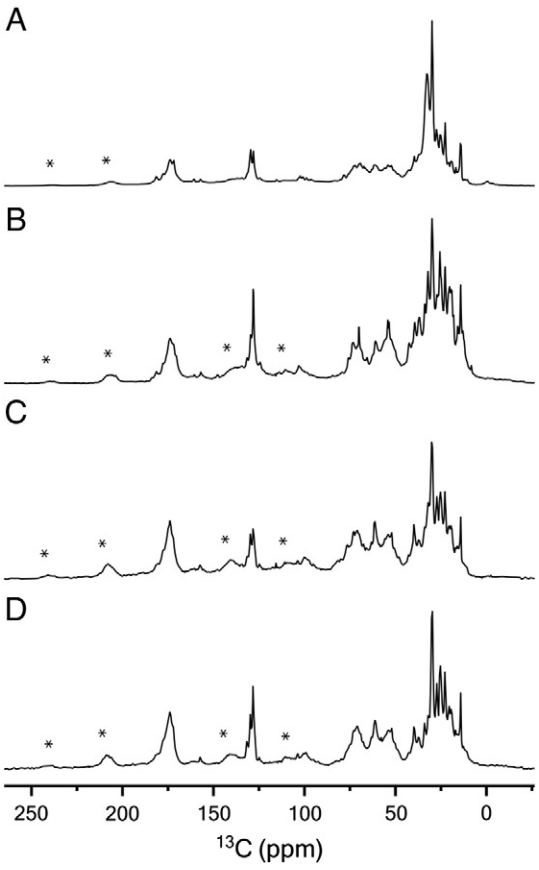

Fig. 1. Quantitative spectra (DP) of ^{13}C labeled (A) *N. oculata*, (B) *P. lutheri*, (C) wild-type and (D) cell-wall depleted *C. reinhardtii*. Spinning side bands are indicated by asterisks.

Overall, the quantitative direct polarization spectra are, as might be expected for whole algal cells, exceedingly crowded. In order to simplify the spectra and, thus, increase resolution, a dynamic filter approach was applied to enhance resonances from mobile or rigid regions using RINEPT and CP, respectively. The resulting spectra are shown in Fig. 2. A major improvement in resolution is observed in the spectra of the mobile regions (Fig. 2, left) which are also considerably simplified, notably for *P. lutheri* and *C. reinhardtii* in which high protein content (30% dry weight) shows significant intensity [37,38]. The RINEPT spectra filter out resonances with short transverse relaxation times, hence the increase in resolution. Most peaks are present in both mobile and rigid regions but with differing intensities. The CP spectra (Fig. 2, right) seem particularly dominated by protein signal as evidenced with the protein-rich *C. reinhardtii* (Fig. 2C). The carbonyl peak (circa 175 ppm) is less intense as compared to the direct polarization spectra displayed in Fig. 1. This could be explained by the fact that CP is less efficient for mobile molecules such as lipids which contribute to the carbonyl peak, and also suggests that proteins are more mobile in the microalgal cells than in a powder or a crystalline sample. This effect is more pronounced for carbons that are not bonded to hydrogens which are harder to cross polarize [33]. A detailed analysis of the different spectral regions is nevertheless possible. This work will focus on the study of carbohydrates and lipids.

3.1. Carbohydrate analysis

Carbohydrate resonances in microalgae are expected from the cell walls, the headgroup of galactolipids abundant in organelles' membranes, as well as the storage polysaccharides. Indeed the marine species studied store sugars in the form of β-(1 → 3) and β-(1 → 6) glycans known as chrysolaminarin [26] while *C. reinhardtii* uses starch grains, both being glucose polymers. As detailed in Table 1, the cell wall composition of *N. oculata*, *P. lutheri* and *C. reinhardtii* is particularly different. It is composed of cellulose in the heterokontophyta *N. oculata*, and contains both cellulose and hemicellulose in the haptophyta *P. lutheri*. Hydroxyproline-rich glycoproteins, to which oligosaccharides bind, are found in the cell wall of the chlorophyta *C. reinhardtii* [17]. More specifically, glucose largely dominates in *N. oculata* (68% by weight) [39] while it only represents 43% of the saccharides in *P. lutheri*, which also comprises mannose and galactose (13%), arabinose (12%) and xylose (10%). Finally, the saccharides in *C. reinhardtii* are galactose (48%), arabinose (29%) and mannose (23%).

The RINEPT spectra of the carbohydrate regions (60–112 ppm) of all phytoplankton species are particularly well resolved and shown in Fig. 3. As will be detailed below, they allow identification of peaks from membrane galactolipids and reserve sugars, and reveal the particular cell wall signature for every species. The peak assignment for both the RINEPT and CP spectra in this spectral region is displayed in Tables 2–4.

N. oculata is protected by a cellulose wall which is not easily digested or degraded [40]. Analysis of the RINEPT and CP spectra of *N. oculata* allows detection of resonances in which chemical shifts (see Table 2) agree with those reported for cellulose and, thus, are assigned to the cell wall. Chemical shifts corresponding to both β-(1 → 3) and β-(1 → 6) glycans are also detected and assigned to chrysolaminarin. The remaining resonances can be ascribed to the galactolipids while those unassigned at ca. 99 ppm can be due to the presence of minor saccharides such as xylose, or glycans (i.e. glucose in the α conformation). While the cellulose anomeric carbon C1 only appears in the rigid (CP) spectrum, the remaining carbons show up in the spectra of both rigid and mobile zones. Similarly, the C2 and C4 resonances of chrysolaminarin are exclusively detected in the CP spectra but the remaining resonances appear on both spectra. Note that there is a resonance overlap for the chrysolaminarin C1 and C2 with galactosyldiglycerides G1 and headgroup carbons, respectively (see Fig. S1 for carbon numbering in lipids).

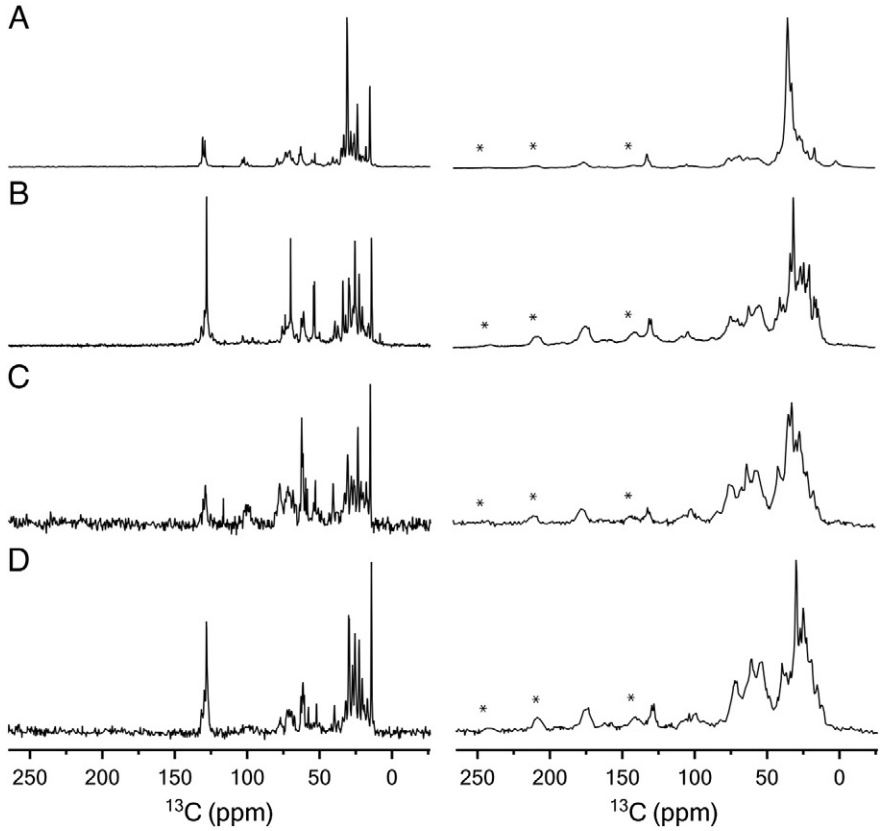

Fig. 2. Dynamically filtered ^{13}C NMR spectra of (A) *N. oculata*, (B) *P. lutheri*, (C) wild-type and (D) cell-wall depleted *C. reinhardtii*. Dynamic and rigid regions detected with RINEPT (left) and cross polarization (right), respectively. Spinning side bands are indicated by asterisks.

The analysis of the carbohydrate region of *P. lutheri* in Table 3 is more complex due to an increased contribution of less abundant saccharides (galactose, mannose and arabinose notably). *P. lutheri* is a golden-brown flagellate which surface is covered by small cellulose grains forming mushroom-like scales [17]. Peaks assigned to cellulose are indeed present in CP and RINEPT spectra, and hemicellulose (xyloglucan) resonances are also detected, consistent with the high amount of galactose and xylose in *Pavlova* [39]. As for *N. oculata*, the presence of the major component of the storage sugar chrysolaminarin (Glu β-(1 → 3)) is also confirmed by our spectra and especially evidenced from the RINEPT spectrum. The remaining resonances can be assigned to arabinan and galactan or galactolipid headgroups. Only two resonances are exclusively present in rigid environments, i.e., the C4 carbon in chrysolaminarin (68.3 ppm) and one at 98.8 ppm that could not be assigned.

In the case of *C. reinhardtii*, the cell wall is composed of hydroxyproline (Hyp)-rich O-glycosylated proteins with mainly arabinosyl/galactosyl sidechains [41]. Recent work by Bollig et al. [42] identifies the Hyp-bound O-glycans as α-D-Gal*f*-(1 → 2)-β-L-Ara*f*-(1 → 2)-β-L-Ara*f*-(1 → 4)Hyp or 3-methyl-β-L-Ara*f*-(1 → 5)-α-D-Gal*f*-(1 → 2)-β-L-Ara*f*-(1 → 2)-β-L-Ara*f*-(1 → 4)Hyp. While a complete assignment of such oligosaccharides is not available, we compared our results with literature values of the corresponding saccharides (α-D-Gal*f* and β-L-Ara*f*) and methyl glycosides ((CH$_3$)-α-D-Gal*f* and (CH$_3$)-β-L-Ara*f*). We could indeed identify these Hyp-bound glycans, and the proposed assignment is shown in Table 4. Resonances of the O-glycans from glycosylated proteins predominate in the RINEPT spectrum, consistent with the fact that they are more mobile than proteins to which they are attached [43]. When compared to wild-type *C. reinhardtii*, the ^{13}C SS-NMR spectra of the CW15 strain show disappearance or major decrease in intensity of the carbohydrate resonances (Fig. 3, D). These results support that CW15 is not entirely deprived of a cell wall [18]. In addition to these cell-wall resonances, peaks were also assigned to galactolipid sugar or glycerol carbons mostly from the RINEPT spectrum (Table 4). Interestingly, several peaks present in the CP spectra have been assigned to amylose, in agreement with expected rigidity of starch stored in grains inside *Chlamydomonas* cells.

The dynamic filter could not entirely separate the carbohydrate signals from different constituents of the various microalgal cell compartments. However, it provided sufficient selectivity to evidence the differences in the cell wall composition of the microalgae, and revealed the considerable complexity in the cellulose forms which compose the cell wall of *P. lutheri*. The cell wall and storage sugars appear to have an intermediate mobility with carbons that can be considered as rigid from an NMR perspective while others are mobile. Chrysolaminarin accumulates in solution in vacuoles inside the cell, which could explain its relative mobility [26], while glucose peaks from starch grains were better identified in the CP spectrum of *C. reinhardtii*, indicating a more rigid behavior. Resonances which could be exclusively assigned to galactolipids were only distinguished in the RINEPT spectrum. There is some overlap between cell wall, galactolipids and storage carbohydrate resonances; however they could be easily distinguishable if their dynamics are taken into account by enhancing selectivity using additional filtering steps, for example in a 2D spectrum. Using 2D methods coupled with dynamic filters such as those described for the study of bacteria [44] or plant cell walls [45], carbohydrates in these three environments (cell wall, storage and membrane) should be fully distinguishable and are currently being studied using this approach.

3.2. Fatty acids and lipid analysis

Lipid composition in vegetal cells is very different from that of animals'. Phosphatidylcholine (PC), phosphatidylserine (PS) and phosphatidylethanolamine (PE) are dominant in animal cells,

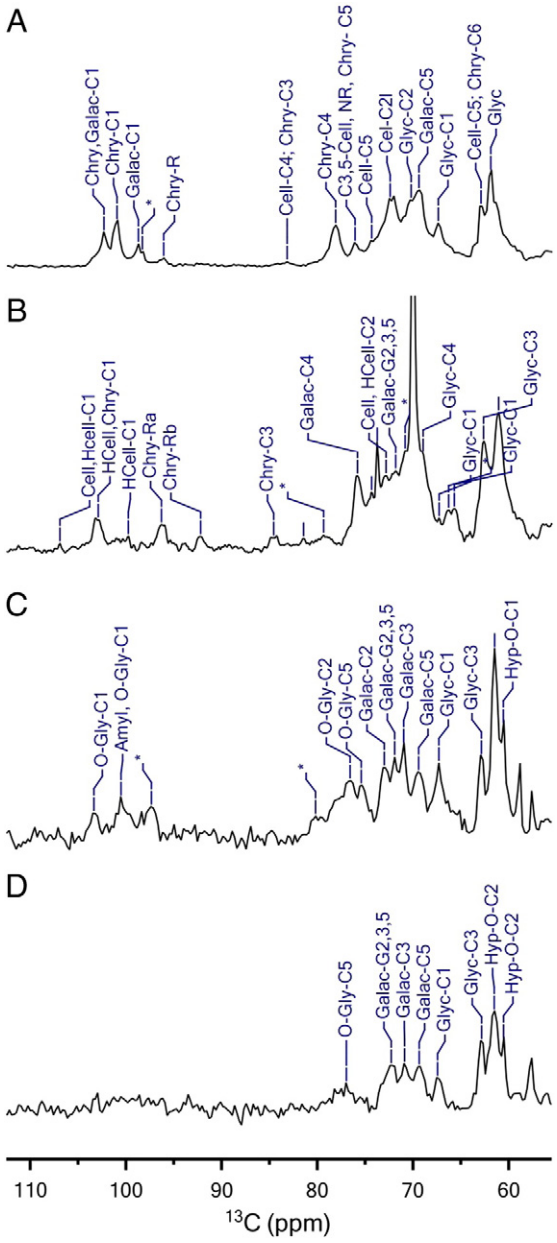

Fig. 3. Comparison of the hydrocarbon regions of (A) *N. oculata*, (B) *P. lutheri*, (C) wild-type and (D) cell-wall depleted *C. reinhardtii* detected with RINEPT. Abbreviations are Cell: Cellulose, HCell: Hemicellulose, Chry: Chrysolaminarin, Galac: Galactosyl in galactolipids, O-Gly: Glycans in Hyp-rich cell wall glycoprotein, Hyp-O: Hydroxyproline in Hyp-rich cell wall protein, Glyc: Glycerol in galactolipids. Unassigned peaks are marked with an asterisk.

while phosphatidylglycerol (PG) and glycolipids (mono- and digalactosyldiglycerides, MGDG and DGDG) are the most abundant in green plant cells. Sulfolipids and betaine lipids are also common in microalgae. The most abundant lipid structures in the microalgae studied are illustrated in Fig. S1. The FA chain composition is also markedly different. In animal cells, saturated palmitoyl (C16:0) and stearoyl (C18:0), and unsaturated oleoyl (C18:1), linoleoyl (C18:2) and arachidonoyl (20:4) lipid chains are mostly found, while PUFA chains dominate in vegetal cells [21]. As for carbohydrates, lipids in microalgae are used both for reserve and structure purposes. Triacylglycerides (TAGs) are stored in vacuoles while phospholipids and glycolipids are the membrane building blocks [22,46]. The fluidity of membranes is determined by the polar headgroup and mostly by the saturation level of the FA chains. Glycolipids and sulfolipids are almost exclusively found in organelle membranes such as the chloroplast, whereas most phospholipids – except for PG – and betaine lipids are found in non-plastid membranes [47].

The hydrophobic region of the membranes – either from the plasmalemma or the organelles – can be probed by monitoring the resonances of lipid headgroups and FA chains. In all spectra, the most intense peak is at 29.8 ppm readily assigned to CH_2 groups in FAs and lipids (Table S1–S3). This does not necessarily reflect a higher proportion of lipids with respect to other constituents since, for instance, *N. oculata* and *P. lutheri* comprise twice as much proteins than lipids [39]. The particularly intense peak at 29.2 ppm comes from the contribution of all the CH_2 groups in FAs that will resonate at the same frequency, whereas protein resonances will be distributed over a larger range of chemical shifts. However, some characteristic resonances can be used to monitor changes in the FA profile. On all spectra, a peak is present at 14.2 ppm which is assigned to the terminal CH_3 groups of FAs, whether saturated or not (Table S1). The intensity ratio between the CH_2 and terminal CH_3 resonances could thus be used to monitor changes in the FA length under an external stress, provided that the number of double bonds remains constant. Double bonds in FAs are reported from 127.8 to 129.6 ppm [6,9,48] and changes in the number of double bonds can be monitored by the ratio between the main CH_2 peak at 29.8 ppm and the region of the double bonds. However, care would have to be taken in interpreting such results since some intensity in this region will result from the presence of pigments, although their contribution will be minor [49].

Nannochloropsis microalgae have been used in aquaculture for more than two decades to feed fish and shell fish larvae because of their high content in eicosapentaenoic acid (EPA or C20:5 (n-3)) [23,24]. They are yellow-green eustigmatophytes classified as picoplankton because of their small diameter (2–4 μm). The total lipid content in *N. oculata* varies between 25 and 32% (dry weight) but was found higher (40%) in other studies [24]. More specifically, 25% galactolipids, 22% phospholipids and 8% TAGs are typically found [25]. MGDG and DGDG, which together represent about 45% of the polar lipids, are mainly found in the membranes of organelles such as the thylakoid membrane of chloroplasts [23]. Carbon wax and sterol esters – mainly cholesterol – were also reported [23]. PC is the most abundant phospholipid, but PG, PE and PI are also found, albeit in lower proportions [23]. The presence of the sulfolipid sulfoquinovosyl-diacylglycerol (SQDG) and the betaine lipid diacylglyceryl-trimethylhomoserine (DGTS) was also reported in this alga [23].

The peak assignment shown in Table S1 confirms the presence of galactosyldiacylglycerols. Peaks characteristic of the SQDG sugar head group seem present on both the CP and RINEPT spectra, but ambiguous because of the overlap with carbons from MGDG or PC headgroup, except for G1 at ~99 ppm. The sugar moieties are better evidenced on the RINEPT spectrum while the glycerol moieties appear better in the CP spectrum. The use of a dynamic filter allows isolating the peaks from PC, dominant in the plasma membrane. Resonances assigned to PC such as the C1 of the acyl chains (~173.7 ppm), the C_α (60.7 ppm) or the characteristic trimethylamine at 54 ppm are identified on the spectra.

The FA chain composition in *N. oculata* is dominated by C16:0, C16:1 and EPA which altogether account for more than 60% of the total FAs mass [19,24]. In terms of total FA composition, 21% of the chains are saturated, 30% are monosaturated and 40% are PUFAs [25]. Most of the EPA is accumulated in TAGs inside the cell [19]. Of course the FA profile could vary with salinity, temperature, and other growth conditions (auxotrophic, etc.) [50,51]. The CP and RINEPT spectra are dominated by lipids' methylene signal (30–33 ppm) consistent with the high content in saturated and mono-unsaturated FA chains. The RINEPT spectrum also shows a strong signal at 128–130 ppm consistent with the high proportion of PUFAs, and possibly to EPA from the vacuolar and mobile TAGs.

P. lutheri is used in aquaculture as food for fish, crustaceans and mollusks larvae because it accumulates PUFAs [27,28]. This species has a different lipid profile compared to the picoplanktonic *N. oculata*

Table 2
^{13}C chemical shifts in the carbohydrate region (60–112 ppm) of *Nannochloropsis oculata* using cross polarization (rigid) or RINEPT (mobile) experiments. Assignments according to literature values.

Rigid	Mobile	Cell wall		Storage sugars (chrysolaminarin)[a]				Membranes[b]	
		Cellulose [45]		β-D-(1 → 3) glucan [54]		Glu(1 → 6) [55]		Galactosyl [56,57]	
δ (ppm)	δ (ppm)	δ (ppm)	Cn	δ (ppm)	Cn	δ (ppm)	Cn	δ (ppm)	Cn
106.0		105.0	C1						
102.3	102.4			102.7–102.8	C1			102.5	G1
	101.0					100.8–101.8	C1		
98.8	98.8							99.4	G1
	98.4	–	–	–	–	–	–	–	–
96.5	96.1			92.3–95.9	Rα				
83.2	83.2	85.0	C4	84.0–84.4	C3	83.2–83.5	C3		
78.2	78.1					77.4–77.7	C4		
	76.1	75.3	C3, C5	75.8–76.1	NR, C5	73.2–75.8	C5		
	74.4					73.2–75.8			
73.0				73.6–74.1	C2	72.8–73.2	C2	73.1–74.0	G2,3,5
	72.5	72.7	C2			72.8–73.2	C2		
	70.3								Glyc C2
	69.4			69.0				69.7	G5
68.2				68.3	C4			68.8	G4,5
	67.4							67.7	Glyc C1
66.0		–	–	–	–	–	–	–	–
	63.0	62.5	C6			61.9–63.2	C6		
	62.0			62.0					
	61.2			60.9	C6			62.1	G6

[a] Rα = reducing-end signal α, Rβ = reducing-end signal β, NR = non-reducing-end signal.
[b] Galactosyl part of MGDG and DGDG; Glyc = glycerol.

(Table 1), and is not as rich in lipids since it contains about 17% (dry weight) of lipids in the stationary phase [37]. This includes about 40% TAG, 28% MGDG, 10% SQDG, 8% DGDG, 6% betaine lipids and 4% PG [28]. Eichenberger and Gribi [29] report 42% TAG, 19% MGDG, 12% DGDG, 9% SQDG, 1% PG, 2% diacylglyceryl glucuronide (DGGA), 6% diacylglyceryl hydroxymethyl-N,N,N-trimethyl-β-alanine (DGTA) and 5% diacylglyceryl carboxyhydroxymethylcholine (DGCC) but these profiles depend on the growth phase of the cells. The rest is made of unknown FAs or lipid molecules [19,27] but some groups report the presence of cardiolipin, acylated steryl glucosides, as well as mono- and diacylglycerols (MAG and DAG) and free FAs [27–29]. Thus, the lipid profile of *P. lutheri* is peculiar since it contains a large variety of lipid species. SQDG, the betaine lipids DGCC and DGTA, as well as DGGA are localized in extraplastid membranes [19,29], while MGDG and DGDG are found in the chloroplast [29]. Betaine lipids have a zwitterionic structure similar to PC — a phospholipid that is not detectable in

Table 3
^{13}C chemical shifts in the carbohydrate region (60–112 ppm) of *Pavlova lutheri* using cross polarization (rigid) or RINEPT (mobile) experiments. Assignments according to literature values.

Rigid	Mobile	Cell wall								Storage sugars[a]		Membranes[b]	
		Cellulose [45]		Hemicellulose [45]						(Chrysolaminarin)		Galactosyl [56,57]	
				Glu(1 → 4)		Gal		Xyl		β-D-(1 → 3) glucan [54]			
δ (ppm)	δ (ppm)	δ (ppm)	Cn	δ (ppm)	Cn	δ (ppm)	Cn	δ (ppm)	Cn	δ (ppm)	Cn	δ (ppm)	Cn
106.4	106.9	105.0	C1	105.0	C1								
102.9	102.9					104.0	C1			102.7–102.8	C1		
	99.8							99.7	C1				
98.8		–	–	–	–	–	–	–	–	–	–	–	–
	96.3									95.9	Rα		
	92.2									92.3	Rβ		
85.7	84.6	85.0	C4							84.4	C3		
	81.5	–	–	–	–	–	–	–	–	–	–	–	–
	79.4	–	–	–	–	–	–	–	–	–	–	–	–
76.0	75.8	75.3	C3.5	75.9	C3	76.7	C3			75.8–76.1	NR, C5	75.3	G4
	74.3					74.8	C5	74.4	C3	74.1	C2		
73.6	73.8			73.8	C5	74.0	C2			73.6	C2		
	72.8	72.7	C2	72.7				72.5	C2			73.1	G2,3
	71.8												G2,3
71.1	70.8	–	–	–	–	–	–	–	–	–	–	–	–
	70.0											69.9	G5
	69.0											68.8	G4
68.3										68.3	C4		
	67.3											67.7	Glyc C1
66.5	66.3	–	–	–	–	–	–	–	–	–	–	–	–
65.7	65.6											66.0	Glyc C1
	62.6	62.5	C6					62.3	C5				Glyc C3
61.0	61.1			61.5	C6	61.7	C6			60.9	C6		G6

[a] Rα = reducing-end signal α, Rβ = reducing-end signal β, NR = non-reducing-end signal.
[b] Galactosyl part of MGDG, DGDG and SQDG; Glyc = glycerol.

Table 4
^{13}C chemical shifts in the carbohydrate region (60–112 ppm) of *Chlamydomonas reinhardtii* using cross polarization (rigid) or RINEPT (mobile) experiments. Assignments according to literature values.

Rigid	Mobile	Cell wall										Storage sugars		Membranes[a]	
		β-L-Araf-[42]		(CH_3)-β-L-Araf-[58]		α-D-Galf-[59]		(CH_3)-α-D-Galf [58]		Hyp-O-glycan [42]		Starch (amylose) [60]		Galactosyl [56,57]	
δ (ppm)	δ (ppm)	δ (ppm)	Cn	δ (ppm)	Cn	δ (ppm)	Cn	δ (ppm)	Cn	δ (ppm)	Cn	δ (ppm)	Cn	δ (ppm)	Cn
	103.3			103.2	C1	103.5	C1	103.1	C1					103.4	G1
100.3	100.5	99.3–101.9	C1									100.9	C1	99.4	G1
	97.3	–	–	–	–	–	–	–	–	–	–	–	–	–	–
82.1				83.1	C4	82.7	C4	82.3	C4			78.6	C4		
	80.2	–	–	–	–	–	–	–	–	–	–	–	–	–	–
	79.6									78.6	C4				
	76.6			77.5	C2	77.8	C2	77.4	C2						
	75.4			75.7	C3	75.9	C3	75.5	C3					75.3	G4
73.6								73.7	C5			74.6	C3		
	73.0													72.9–73.1	G2
72.0	71.9											72–73	C2,5	–	G2,3,5
	71.0													71.1	G3
	69.4													69.7	G5
	67.3													67.7	Glyc C1
64.9		64.2	C5	64.2	C5										
	62.9					63.8	C6	63.4	C4						Glyc C3
61.5	61.5									61.7–61.9	C2	61.9	C6		
	60.6									61.1	C2				

[a] Galactosyl part of MGDG, DGDG and SQDG; Glyc = glycerol.

P. lutheri [29]. DGCC is believed to be involved in the transfer of FAs from the cytoplasm to the chloroplast and, thus, in the biosynthesis of MGDG [29]. Because the relative proportion of betaine lipids as well as PUFAs increases at low temperature, they are believed to modulate the adaptation of *P. lutheri* at low temperature [29].

The ^{13}C SS-NMR analysis of whole *P. lutheri* cells shows several peaks that can be assigned to MGDG and SQDG between 60 and 103 ppm, particularly evident on the RINEPT spectrum (Table S2). The use of the dynamic filter also allows identification of betaine lipids from the plasmalemma in the RINEPT spectrum from the characteristic headgroup carbons at ~40 and 54 ppm. The natural occurrence of the other lipids is possibly too low to allow their identification.

P. lutheri possesses very long-chain PUFAs (>C20) which are mainly accumulated in MGDG (45% of the total FAs) and TAG (33% of the total FAs) [19,27]. More specifically, EPA dominates in MGDG and TAG while docosahexaenoic acid (DHA or C22:6 (n-3)) is found in several lipid classes, and especially betaine lipids [27,47]. Oleate, docosapentaenoic and DHA predominate in DGGA while DGCC is enriched in palmitate and EPA [19]. It is noteworthy that C14:0, C16:0 and C:16:1 are abundant in *P. lutheri*, representing about 56% of the FA chains when cells are grown at 20 °C as in our study [28].

Contrary to the lipid-rich *N. oculata* which CP spectrum reveals strong lipid resonances, *P. lutheri*'s spectrum is not dominated by lipid resonances, in agreement with its lower lipid content. While lipid resonances are assigned in both the CP and RINEPT spectra, they are better evidenced with the RINEPT experiment from which the CH_3 (14.2 ppm), allylic or saturated carbons (20.6–33.9 ppm) stand out. Moreover, the presence of long-chain PUFAs is confirmed from the strong peak at 128 ppm ascribed to olefin carbons dominating the RINEPT spectrum (Table S2).

Glycolipids are the most abundant in *C. reinhardtii*. Indeed, Vieler et al. report 38% MGDG, 24% DGDG, 12% SQDG, 10% PG, 3% PE and 12% DGTS [21]. Glycolipids actually represent 70–80% of the total lipid content of thylakoid membranes, completed by DGTS and PG in equal proportions [52]. The major plasma membrane lipid is the betaine lipid DGTS [19,21], therefore the PC content is expected to be low. Indeed, PC is not found in this alga, but phosphatidylinositol (PI) is present in small amounts [19]. Cardiolipin, carotenoids and sterols (ergosterol and 7-dehydroporiferasterol) are also accounted for in the lipid content [18].

In agreement with the reported lipid profile of *C. reinhardtii*, the ^{13}C resonance of the abundant glycolipids and sulfolipids can be detected in both RINEPT and CP spectra; however the headgroups are better evidenced in the RINEPT spectrum (Table S3). The presence of DGTS from the plasma membrane was confirmed with the characteristic trimethyl peak at ~54 ppm, especially strong (50% relative abundance) on the RINEPT spectrum. Peaks assigned to Hyp-bound glycans are also identified at 37.6, 52.1 and 61.5 ppm in the RINEPT spectrum, in agreement with the mobility previously observed for these saccharides in the carbohydrate region.

Contrarily to *Nannochloropsis* and *Pavlova*, *C. reinhardtii* WT contains only traces of EPA and DHA, the most abundant FA chains being C16 and C18. MGDG and DGDG mainly contain unsaturated C18 while sulfolipids have a greater proportion of saturated C16 [18,53]. This FA chain profile is typical of freshwater species which, like terrestrial plants, is stopped at linoleic (LOA, C18:2) and linolenic (LNA, 18:3) acids [20,22]. Such profile can easily be seen with the intense methylene-related resonances between 29 and 32 ppm (see Table S3) in both the CP and RINEPT spectra. The olefin carbon signals from PUFAs (~128 ppm) are correspondingly low comparatively to the two marine species. Differences in the olefin and methylene peak relative intensities are seen for *C. reinhardtii* CW15 strain in Fig. 2D, suggesting a different profile, perhaps to compensate the partial lack of a cell wall, but this needs to be further investigated.

In summary for this section, ^{13}C-SS-NMR with MAS and a dynamic filter could not sort microalgal cell fatty acid and lipid components owing to their dynamics, but allowed identification of lipid components from the plasmalemma, organelle membranes, as well as TAG reserve.

4. Conclusion

This work is a comparative 1D ^{13}C SS-NMR study of whole microalgae cells with the objective of determining whether the signals from the surface of these organisms, i.e., the cell walls and the plasmalemma membrane, can be spectroscopically isolated. Our results showed that dynamical heterogeneity could not allow distinguishing all membrane or cell wall components which seem to have some level of mobility. Indeed, cellulosic cell walls protecting microalgae such as *N. oculata* and *P. lutheri* are known to be viscoelastic and hard to break [40]. However, the use of CP and RINEPT filter combined to the facile

isotopic labeling with $NaH^{13}CO_3$ could reveal differences in the mobility of some microalgal constituents such as the storage lipids and sugars. It also showed to be a useful strategy to reveal differences in the composition and organization of intact microalgae. The strong spectral overlap and low resolution observed in a normal (DP) spectrum could be partially overcome by using experiments which favor mobile or rigid regions. The resulting high resolution, especially on the RINEPT spectra, enabled identification of components (carbohydrates and lipids) not only from the cell surface but also from the organelle membranes, storage lipids and sugars of the three species studied. The CP spectra appear to be more useful to study protein components. Together, these experiments enabled the identification of most of the constituents expected in phytoplankton cells. They should also enable the study of the interaction of contaminants. The dynamical selectivity used in this work will have to be extended to 2D methods to allow a complete characterization of microalgal cell components.

Acknowledgements

This work was supported by the Fonds de Développement Académique du Réseau (FODAR) de l'Université du Québec, the Natural Sciences and Engineering Research Council of Canada (NSERC) and the Canada Foundation for Innovation. B.G. is grateful to Ressources Aquatiques Québec (RAQ) and the Training Program in Bionanomachines (NSERC) for the award of scholarships. The authors would like to thank Prof. D. Dewez, Dr. A. Oukarroum and A.L.D.A.G. Da Silva (UQAM) as well as A. Lebas (IBPC) for technical support.

Appendix A. Supplementary data

Supplementary data to this article can be found online at http://dx.doi.org/10.1016/j.bbamem.2014.07.017.

References

[1] A. Richmond, Handbook of Microalgal Culture: Biotechnology and Applied Phycology, Blackwell Science Ltd., Oxford, 2004.
[2] H. Gerken, B. Donohoe, E. Knoshaug, Enzymatic cell wall degradation of *Chlorella vulgaris* and other microalgae for biofuels production, Planta 237 (2013) 239–253.
[3] P. Spolaore, C. Joannis-Cassan, E. Duran, A. Isambert, Commercial applications of microalgae, J. Biosci. Bioeng. 101 (2006) 87–96.
[4] R. Sakthivel, S. Elumalai, M.M. arif, Microalgae lipid research, past, present: a critical review for biodiesel production, in the future, J. Exp. Sci. 2 (2011) 29–49.
[5] L. Catoire, R. Goldberg, M. Pierron, C. Morvan, H. du Penhoat, An efficient procedure for studying pectin structure which combines limited depolymerization and ^{13}C NMR, Eur. Biophys. J. 27 (1998) 127–136.
[6] C.M. Beal, M.E. Webber, R.S. Ruoff, R.E. Hebner, Lipid analysis of *Neochloris oleoabundans* by liquid state NMR, Biotechnol. Bioeng. 106 (2010) 573–583.
[7] M. Bental, M. Oren-Shamir, M. Avron, H. Degani, ^{31}P and ^{13}C-NMR studies of the phosphorus and carbon metabolites in the halotolerant alga, *Dunaliella salina*, Plant Physiol. 87 (1988) 320–324.
[8] B. Tesson, S. Masse, G. Laurent, J. Maquet, J. Livage, V. Martin-Jézéquel, T. Coradin, Contribution of multi-nuclear solid state NMR to the characterization of the *Thalassiosira pseudonana* diatom cell wall, Anal. Bioanal. Chem. 390 (2008) 1889–1898.
[9] M.S. Chauton, T.R. Størseth, J. Krane, High-resolution magic angle spinning NMR analysis of whole cells of *Chaetoceros muelleri* (Bacillariophyceae) and comparison with ^{13}C-NMR and distortionless enhancement by polarization transfer ^{13}C-NMR analysis of lipophilic extracts, J. Phycol. 40 (2004) 611–618.
[10] M. Renault, R. Tommassen-van Boxtel, M.P. Bos, J.A. Post, J. Tommassen, M. Baldus, Cellular solid-state nuclear magnetic resonance spectroscopy, Proc. Natl. Acad. Sci. U. S. A. 109 (2012) 4863–4868.
[11] M. Renault, S. Pawsey, M.P. Bos, E.J. Koers, D. Nand, R. Tommassen-van Boxtel, M. Rosay, J. Tommassen, W.E. Maas, M. Baldus, Solid-state NMR spectroscopy on cellular preparations enhanced by dynamic nuclear polarization, Angew. Chem. Int. Ed. 51 (2012) 2998–3001.
[12] C. Tardy-Laporte, A.A. Arnold, B. Genard, R. Gastineau, M. Morançais, J.L. Mouget, R. Tremblay, I. Marcotte, A ^{2}H solid-state NMR study of the effect of antimicrobial agents on intact *Escherichia coli* without mutating, Biochim. Biophys. Acta 1828 (2013) 614–622.
[13] G. Zandomeneghi, K. Ilg, M. Aebi, B.H. Meier, On-cell MAS NMR: physiological clues from living cells, J. Am. Chem. Soc. 134 (2012) 17513–17519.
[14] H. Takahashi, I. Ayala, M. Bardet, G. De Paëpe, J.-P. Simorre, S. Hediger, Solid-state NMR on bacterial cells: selective cell wall signal enhancement and resolution improvement using dynamic nuclear polarization, J. Am. Chem. Soc. 135 (2013) 5105–5110.
[15] N.V. Kulminskaya, M.Ø. Pedersen, M. Bjerring, J. Underhaug, M. Miller, N.-U. Frigaard, J.T. Nielsen, N.C. Nielsen, In situ solid-state NMR spectroscopy of protein in heterogeneous membranes: the baseplate antenna complex of *Chlorobaculum tepidum*, Angew. Chem. Int. Ed. 51 (2012) 6891–6895.
[16] J. Xu, P. Zhu, M.D. Morris, A. Ramamoorthy, Solid-state NMR spectroscopy provides atomic-level insights into the dehydration of cartilage, J. Phys. Chem. B 115 (2011) 9948–9954.
[17] C. Van den Hoek, D.G. Mann, H.M. Jahns, Algae — An Introduction to Phycology, Cambridge University Press, Cambridge, 1995.
[18] E.H. Harris, The *Chlamydomonas* Sourcebook. Introduction to *Chlamydomonas* and its Laboratory Use, 2nd ed. Elsevier Inc., Amsterdam, 2009.
[19] I.A. Guschina, J.L. Harwood, Lipids and lipid metabolism in eukaryotic algae, Prog. Lipid Res. 45 (2006) 160–186.
[20] V. Mimouni, L. Ulmann, V. Pasquet, M. Mathieu, L. Picot, G. Bougaran, J.-P. Cadoret, A. Morant-Manceau, B. Schoefs, The potential of microalgae for the production of bioactive molecules of pharmaceutical interest, Curr. Pharm. Biotechnol. 13 (2012) 2733–2750.
[21] A. Vieler, C. Wilhelm, R. Goss, R. Süß, J. Schiller, The lipid composition of the unicellular green alga *Chlamydomonas reinhardtii* and the diatom *Cyclotella meneghiniana* investigated by MALDI-TOF MS and TLC, Chem. Phys. Lipids 150 (2007) 143–155.
[22] P.J.L.B. Williams, L.M.L. Laurens, Microalgae as biodiesel & biomass feedstocks: review & analysis of the biochemistry, energetics & economics, Energy Environ. Sci. 3 (2010) 554–590.
[23] A. Sukenik, Production of eicosapentanoic acid by the marine eustigmatophyte *Nannochloropsis*, in: Z. Cohen (Ed.), Chemicals From Microalgae, Tayor & Francis Ltd., London, 1999, pp. 41–53.
[24] N. Gu, Q. Lin, G. Li, Y. Tan, L. Huang, J. Lin, Effect of salinity on growth, biochemical composition, and lipid productivity of *Nannochloropsis oculata* CS 179, Eng. Life Sci. 12 (2012) 631–637.
[25] P. Hodgson, R.J. Henderson, J. Sargent, J. Leftley, Patterns of variation in the lipid class and fatty acid composition of *Nannochloropsis oculata* (Eustigmatophyceae) during batch culture, J. Appl. Phycol. 3 (1991) 169–181.
[26] E. Corteggiani Carpinelli, A. Telatin, N. Vitulo, C. Forcato, M. D'Angelo, R. Schiavon, A. Vezzi, G.M. Giacometti, T. Morosinotto, G. Valle, Chromosome scale genome assembly and transcriptome profiling of *Nannochloropsis gaditana* in nitrogen depletion, Mol. Plant (2013), http://dx.doi.org/10.1093/mp/sst120.
[27] L.A. Meireles, A.C. Guedes, F.X. Malcata, Lipid class composition of the microalga *Pavlova lutheri*: eicosapentaenoic and docosahexaenoic acids, J. Agric. Food Chem. 51 (2003) 2237–2241.
[28] H. Tatsuzawa, E. Takizawa, Changes in lipid and fatty acid composition of *Pavlova lutheri*, Phytochemistry 40 (1995) 397–400.
[29] W. Eichenberger, C. Gribi, Lipids of *Pavlova lutheri*: cellular site and metabolic role of DGCC, Phytochemistry 45 (1997) 1561–1567.
[30] R.R.L. Guillard, Culture of phytoplankton for feeding marine invertebrates, in: W.L. Smith, M.H. Chanley (Eds.), Culture of Marine Invertebrate Animals, Plenum Press, New York, 1975, pp. 29–60.
[31] D.S. Gorman, R.P. Levine, Cytochrome f and plastocyanin: their sequence in the photosynthetic electron transport chain of *Chlamydomonas reinhardtii*, Proc. Natl. Acad. Sci. U. S. A. 54 (1965) 1665–1669.
[32] J.D. Gross, P.R. Costa, J.P. Dubacq, D.E. Warschawski, P.N. Lirsac, P.F. Devaux, R.G. Griffin, Multidimensional NMR in lipid systems. Coherence transfer through *J* couplings under MAS, J. Magn. Reson. B 106 (1995) 187–190.
[33] D.E. Warschawski, P.F. Devaux, Polarization transfer in lipid membranes, J. Magn. Reson. 145 (2000) 367–372.
[34] D.E. Warschawski, P.F. Devaux, ^{1}H-^{13}C polarization transfer in membranes: a tool for probing lipid dynamics and the effect of cholesterol, J. Magn. Reson. 177 (2005) 166–171.
[35] R. Purusottam, G. Bodenhausen, P. Tekely, Quantitative one- and two-dimensional ^{13}C spectra of microcrystalline proteins with enhanced intensity, J. Biomol. NMR 57 (2013) 11–19.
[36] R.L. Johnson, K. Schmidt-Rohr, Quantitative solid-state ^{13}C NMR with signal enhancement by multiple cross polarization, J. Magn. Reson. 239 (2014) 44–49.
[37] M.R. Brown, C.D. Garland, S.W. Jeffrey, I.D. Jameson, J.M. Leroi, The gross and amino acid compositions of batch and semi-continuous cultures of *Isochrysis* sp. (clone T.ISO), *Pavlova lutheri* and *Nannochloropsis oculata*, J. Appl. Phycol. 5 (1993) 285–296.
[38] K. Roberts, Crystalline glycoprotein cell walls of algae: their structure, composition and assembly, Philos. Trans. R. Soc. Lond. B 268 (1974) 129–146.
[39] M.R. Brown, The amino-acid and sugar composition of 16 species of microalgae used in mariculture, J. Exp. Mar. Biol. Ecol. 145 (1991) 79–99.
[40] C. Safi, M. Charton, O. Pignolet, F. Silvestre, C. Vaca-Garcia, P.-Y. Pontalier, Influence of microalgae cell wall characteristics on protein extractability and determination of nitrogen-to-protein conversion factors, J. Appl. Phycol. 25 (2013) 523–529.
[41] P.J. Ferris, J.P. Woessner, S. Waffenschmidt, S. Kilz, J. Drees, U.W. Goodenough, Glycosylated polyproline II rods with kinks as a structural motif in plant hydroxyproline-rich glycoproteins, Biochemistry 40 (2001) 2978–2987.
[42] K. Bollig, M. Lamshöft, K. Schweimer, F.-J. Marner, H. Budzikiewicz, S. Waffenschmidt, Structural analysis of linear hydroxyproline-bound O-glycans of *Chlamydomonas reinhardtii*—conservation of the inner core in *Chlamydomonas* and land plants, Carbohydr. Res. 342 (2007) 2557–2566.
[43] M.R. Wormald, R.A. Dwek, Glycoproteins: glycan presentation and protein-fold stability, Structure 7 (1999) R155–R160.
[44] T. Kern, M. Giffard, S. Hediger, A. Amoroso, C.c. Giustini, N.K. Bui, B. Joris, C. Bougault, W. Vollmer, J.-P. Simorre, Dynamics characterization of fully hydrated bacterial cell walls by solid-state NMR: evidence for cooperative binding of metal ions, J. Am. Chem. Soc. 132 (2010) 10911–10919.

[45] M. Dick-Pérez, Y. Zhang, J. Hayes, A. Salazar, O.A. Zabotina, M. Hong, Structure and interactions of plant cell-wall polysaccharides by two- and three-dimensional magic-angle-spinning solid-state NMR, Biochemistry 50 (2011) 989–1000.
[46] M. Olofsson, T. Lamela, E. Nilsson, J.P. Bergé, V. del Pino, P. Uronen, C. Legrand, Seasonal variation of lipids and fatty acids of the microalgae *Nannochloropsis oculata* grown in outdoor large-scale photobioreactors, Energies 5 (2012) 1577–1592.
[47] G.A. Thompson Jr., Lipids and membrane function in green algae, Biochim. Biophys. Acta 1302 (1996) 17–45.
[48] S. Everts, J.H. Davis, ^{1}H and ^{13}C NMR of multilamellar dispersions of polyunsaturated (22:6) phospholipids, Biophys. J. 79 (2000) 885–897.
[49] M.R. Brown, S.W. Jeffrey, Biochemical composition of microalgae from the green algal classes Chlorophyceae and Prasinophyceae. 1. Amino acids, sugars and pigments, J. Exp. Mar. Biol. Ecol. 161 (1992) 91–113.
[50] C.V. González-López, M.C. Cerón-García, J.M. Fernández-Sevilla, A.M. González-Céspedes, J. Camacho-Rodríguez, E. Molina-Grima, Medium recycling for *Nannochloropsis gaditana* cultures for aquaculture, Bioresour. Technol. 129 (2013) 430–438.
[51] Q. Lin, N. Gu, G. Li, J. Lin, L. Huang, L. Tan, Effects of inorganic carbon concentration on carbon formation, nitrate utilization, biomass and oil accumulation of *Nannochloropsis oculata* CS 179, Bioresour. Technol. 111 (2012) 353–359.
[52] E.H. Harris, The *Chlamydomonas* Sourcebook: A Comprehensive Guide to Biology and Laboratory Use, Academic Press Inc., San Diego, 1989.
[53] D.R. Janero, R. Barrnett, Cellular and thylakoid-membrane glycolipids of *Chlamydomonas reinhardtii* 137+, J. Lipid Res. 22 (1981) 1119–1125.
[54] T.R. Størseth, K. Hansen, J. Skjermo, J. Krane, Characterization of a β-D-(1 → 3)-glucan from the marine diatom *Chaetoceros mülleri* by high-resolution magic-angle spinning NMR spectroscopy on whole algal cells, Carbohydr. Res. 339 (2004) 421–424.
[55] N. Loening, T. Kanemitsu, P. Seeberger, R. Griffin, Solid-phase synthesis and ^{1}H and ^{13}C high-resolution magic angle spinning NMR of ^{13}C-labeled resin-bound saccharides, Magn. Reson. Chem. 42 (2004) 453–458.
[56] V. Castro, S.V. Dvinskikh, G. Widmalm, D. Sandström, A. Maliniak, NMR studies of membranes composed of glycolipids and phospholipids, Biochim. Biophys. Acta 1768 (2007) 2432–2437.
[57] L.M. de Souza, M. Iacomini, P.A.J. Gorin, R.S. Sari, M.A. Haddad, G.L. Sassaki, Glyco- and sphingophosphonolipids from the medusa *Phyllorhiza punctata*: NMR and ESI-MS/MS fingerprints, Chem. Phys. Lipids 145 (2007) 85–96.
[58] P. Gorin, M. Mazurek, Further studies on the assignment of signals in ^{13}C magnetic resonance spectra of aldoses and derived methyl glycosides, Can. J. Chem. 53 (1975) 1212–1223.
[59] J.H. Bradbury, G.A. Jenkins, Determination of the structures of trisaccharides by ^{13}C-N.M.R. spectroscopy, Carbohydr. Res. 126 (1984) 125–156.
[60] M. Gidley, S. Bociek, ^{13}C CP/MAS NMR studies of amylose inclusion complexes, cyclodextrins, and the amorphous phase of starch granules: relationships between glycosidic linkage conformation and solid-state ^{13}C chemical shifts, J. Am. Chem. Soc. 110 (1988) 3820–3829.

Supplementary material for

DETECTION OF LIPIDS AND SACCHARIDES CONSTITUENTS OF WHOLE MICROALGAL CELL BY ^{13}C SOLID-STATE NMR

Alexandre A. Arnold[1], Bertrand Genard[1], Francesca Zito[2], Réjean Tremblay[3], Dror Warschawski[2] & Isabelle Marcotte[1]*

[1] Department of Chemistry, Université du Québec à Montréal, and Ressources Aquatiques Québec, P.O. Box 8888, Downtown Station, Montréal, Canada, H3C 3P8
[2]Laboratoire de Biologie Physico-Chimique des Protéines Membranaires, CNRS, Université Paris Diderot and Institut de Biologie Physico-Chimique, 13 rue Pierre et Marie-Curie, 75005 Paris, France
[3]Institut des Sciences de la Mer, Université du Québec à Rimouski, and Ressources Aquatiques Québec, 310 Allée des Ursulines, Rimouski, Québec G5L 3A1, Canada

*To whom correspondence should be addressed. Email: marcotte.isabelle@uqam.ca

Figure S1. Structures of microalgae lipids and examples of carbon numbering.

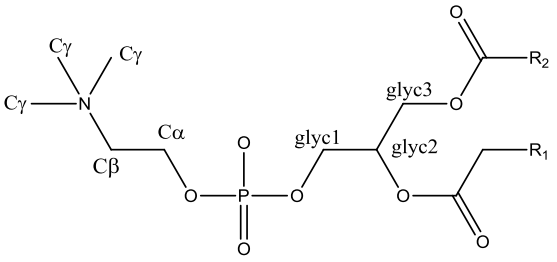

Phosphatidylcholine, carbons on aliphatic chains are numbered starting at the ester bond.

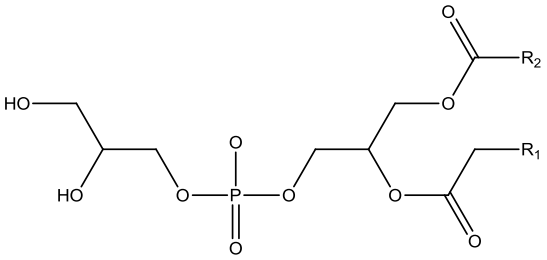

Phosphatidylglycerol.

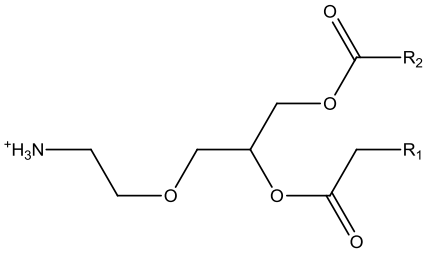

Phosphatidylethanolamine.

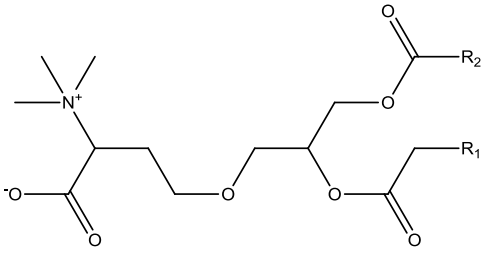

DGTS or betaine lipids (1,2-diacylglyceryl-3-O-4'-[N,N,N-trimethyl]-homoserine).

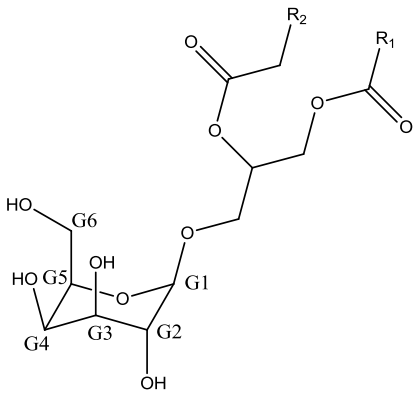

MGDG (monogalactosyl-diacylglycerol).

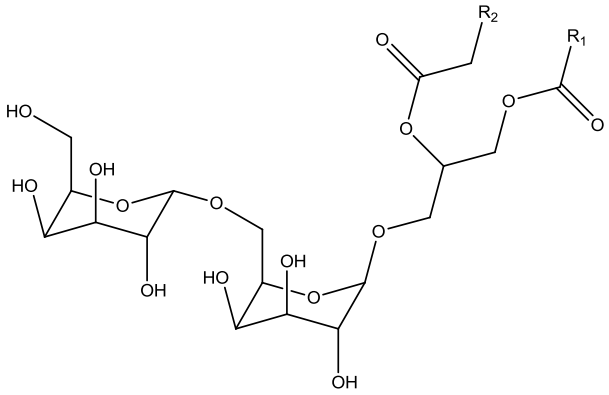

DGDG (digalactosyl-diacylglycerol).

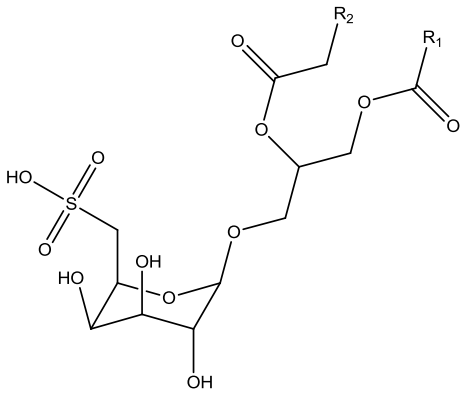

SQDG (sulfoquinovosyldiacylglycerol).

Table S1: ^{13}C chemical shifts and relative intensity of lipids peaks obtained for *Nannochloropsis oculata* by cross-polarization (rigid) or RINEPT (mobile) experiments. Assignments according to literature values.

Rigid zones (CP)		Mobile zones (RINEPT)		Literature values
δ (ppm)	%	δ (ppm)	%	
181.7	1			
173.7	4			Phospholipid, PC chain C1 (173.4 ppm) [1,2]
163.0	1			
157.0	1			
130.0	10	129.7	19	C=C from: glyceryl trioleate (129.5 ppm) [3]; 16:1 C9 or C10; EPA C5 or C6 (129.6-130.1 ppm) [1]; EPA (127.1-129.2 ppm) [4]
128.0	2	128.1	16	C=C from: FA (127.4-128.4 ppm) [5], FA (127.8-127.9 ppm) [3], EPA C11, C14 (127.6-127.9 ppm) [1], MGDG (127 ppm) [6], EPA (127.1-129.2 ppm) [4]
124.4	1			
115.3	1			
106.5	1			
102.5	2	102.4	5	MGDG G1 (104 ppm) [7]
		101.1	6	
99.2	1	98.7	3	SQDG G1 (99.4 ppm) [6]
96.3	1	96.1	1	
83.2	1	83.2	1	
78.6	1	78.2	6	
		76.1	4	
73.6	6			MGDG G5 (74.0 ppm) [7] or SQDG G2 (73.1 ppm) or G3 (73.9 ppm) [6]
		72.2	11	MGDG G3 (72 ppm) [7]
		69.5	13	MGDG Glyc C2 (69.9 ppm) or SQDG G5 (69.7 ppm) [6];
68.7	4			Glyc C2 (68.8-69.0 ppm) [1,3] MGDG G4 (68.8 ppm) [6]; PC Cα (68.4 ppm) [8]
		67.4	7	MGDG Glyc C1 (67.7 ppm) [6]
66.0	6			PC Cβ (66.0 ppm) [5]; PE CH_2N+ (66.3-66.5 ppm) [3]; SQDG Glyc C1 (66.0 ppm) [6]
		61.9	14	Glyc C1,C3 (60.0-62.2 ppm) [1,3]; MGDG G6 or Glyc C3 (62.1 ppm) [6,7]
60.7	5			PC Cα (60.7-60.8 ppm) or Glyc C1,C3 (60.0-62.2 ppm) [1,3]; PC Cα (60.3 ppm) [2]
53.5	5	54.2	5	PC Cγ (54.0 ppm) [5], (54.8 ppm) [2], (54.9 ppm) [8]
		52.2	7	
43.3	2	42.9	3	
39.6	6	39.8	7	
37.3	2	37.0	14	
		32.8	6	FA chain CH_2 from: PC C12 (33 ppm)[2]; MGDG (23.0-35.5 ppm) or SQDG (22.7-34.6 ppm) [6]
32.8	100	32.1	23	FA chain CH_2 from: n-9 on saturated FAs (32.1-32.2 ppm) [1]; MGDG (23.0-35.5 ppm) or SQDG (22.7-34.6 ppm) [6]
29.9	39	29.9	100	FA chain $(CH_2)n$ (29.9 ppm) [5], (29.3-30.1 ppm) [1]; MGDG (23.0-35.5 ppm) or SQDG (22.7-34.6 ppm) [6]
27.3	14	27.4	26	FA chain allylic CH_2 (-C-C=) (27.1 ppm) [3], (27.3-27.4 ppm) [1]; from EPA (26.4-33.5 ppm) [4]; CH_2 from MGDG (23.0-35.5 ppm) or SQDG (22.7-34.6 ppm) [6]
24.7	15	25.0	24	FA chain =C-C-C= (25.4-25.5 ppm) [3,5]; PC chain C3 (25.9 ppm) [2]; CH_2

				from MGDG (23.0-35.5 ppm) or SQDG (22.7-34.6 ppm) [6]
22.7	13	22.8	40	FA chain C*H_2-CH_3 (22.5-22.6 ppm) [3,5], (22.6-22.8 ppm) [1]; CH_2 from MGDG (23.0-35.5 ppm) or SQDG CH2 (22.7-34.6 ppm) [6]
20.9	4	21.0	11	FA chain CH_2 (20.6 ppm) [1]
19.0	8	19.4	9	
		16.9	14	
14.3	13	14.2	50	FA terminal CH_3: for DHA (14.0 ppm) [5]; (13.8-14.0 ppm) [3]; MGDG and SQDG (14.4 ppm) [6]; PC (14.5 ppm)[2]; EPA (13.8-14.5 ppm) [4]

Table S2: ^{13}C chemical shifts and relative intensity of lipids peaks obtained for *Pavlova lutheri* by cross-polarization (rigid) or RINEPT (mobile). Assignments according to literature values.

Rigid zones (CP)		Mobile zones (RINEPT)		Literature values
δ (ppm)	%	δ (ppm)	%	
173.5	4			Phospholipid chain C1 (173.4 ppm) [1,2]; C1 and C2 (172,7 and 173.2 ppm) [5]
171.1	18			FA C1 (171.6 -172.9 ppm) [3]; Betaine CO (171.8 ppm) [9]
157.0	1			
		132.0	8	C=C from EPA C18 (132.1 ppm) [1]
		131.4	18	C=C from DHA C20 (131.3 ppm) [5]
129.5	22	129.6	22	C=C from: glyceryl trioleate (129.5 ppm) [3]; 16:1 C9 or C10; EPA C5 or C6 (129.6-130.1 ppm) [1]; EPA (127.1-129.2 ppm) [4]
		128.9	15	C=C from EPA C6 (128.9 ppm) [1]; EPA (127.1-129.2 ppm) [4]
128.1	20	128.0	105	C=C from: FA (127.4-128.4 ppm) [1,5], FA (127.8-127.9 ppm) [3], EPA C11, C14 (127.6-127.9 ppm) [1], MGDG (127 ppm) [6], EPA (127.1-129.2 ppm) [4]
		124.2	49	
107.5	1			
102.7	7	103.0	9	MGDG G1 (103.4, 104 ppm) [6,7]
		96.3	16	
86.2	1			
		75.8	21	SQDG G4 (75.3 ppm) [6]
73.5	11	73.2	25	MGDG G2 (72.9 ppm) [6], G5 (74 ppm) [6,7]; SQDG G2 (73.1 ppm) or G3 (73.0 ppm) [6]
		71.6	40	MGDG G3 (72 ppm) [7]
		70.0	54	MGDG Glyc C2 Gly (69.9 ppm) or SQDG G5 (69.7 ppm) [6]
68.1	11	69.0	34	Glyc C2 (68.8-69.0 ppm) [1,3]; MGDG G4 (68.8 ppm) or Glyc C1 (67.7 ppm) [6]; Betaine C2 (68.9 ppm) [9]
65.6	8	66.2	6	choline Cβ (66.0 ppm) [5]; PE CH_2N+ (66.3-66.5 ppm) [3]; SQDG Glyc C1 (66.0 ppm) [6]
		62.7	18	Phospholipid Glyc C1 (62.8 ppm) [5]; MGDG Glyc C3 (63 ppm) [7]
60.8	45	61.1	70	Choline Cα (60.3 ppm) [2]; Glyc C1, C3 (61.7-62.0) ppm) [1,3]; MGDG G6 (60 ppm) [7]
		54.2	31	Betaine $(CH_3)_3$ (54 ppm) [10]; PC Cγ (54.0 ppm) [5], (54.8 ppm) [2], (54.9 ppm) [8]
53.5	11	53.5	29	
		50.0	6	
42.5	14			
		40.7	2	PE CH_2N+ (40.5 ppm) [3]
39.3	48	39.4	26	
36.8	27	37.4	23	
		33.9	62	FA chain CH_2 from: PC C12 (33.8 ppm)[2]; C2α,β (33.5-33.9 ppm)[3], (33.8-34.0 ppm) [1]; EPA C2 (33.4 ppm) [1]; MGDG (23.0-35.5 ppm) or SQDG (22.7-34.6 ppm) [6]; EPA (26.4-33.5 ppm) [4]
32.1	100	32.0	27	FA chain CH_2 from: n-9 on saturated FAs (32.1-32.2 ppm) [1]; EPA (26.4-33.5 ppm) [4]; MGDG (23.0-35.5 ppm) or SQDG (22.7-34.6 ppm) [6]; (31.8-31.9 ppm) [3,5]
30.0	86	29.8	38	FA chain (CH_2)n (29.3-29.9 ppm) [1,5], (29.3-30.1 ppm) [1]; EPA (26.4-33.5 ppm) [4]; MGDG (23.0-35.5 ppm) or SQDG (22.7-34.6 ppm) [6]
		29.2	69	FA chain CH_2 from: EPA (26.4-33.5 ppm) [4]; MGDG (23.0-35.5 ppm) or

				SQDG (22.7-34.6 ppm) [6]
27.2	28	27.2	37	FA chain allylic CH_2 (-C-C=) (27.1 ppm) [3], (27.3-27.4 ppm) [1]; from EPA (26.4-33.5 ppm) [4]; CH_2 from MGDG (23.0-35.5 ppm) or SQDG (22.7-34.6 ppm) [6]
		26.6	14	FA chain CH_2 from: EPA C4 (26.5 ppm) [1]; EPA (26.4-33.5 ppm) [4]; MGDG (23.0-35.5 ppm) or SQDG (22.7-34.6 ppm) [6]
		25.6	100	FA chain allyl (=C-C-C=) (25.4-25.6 ppm) [1,3]; CH_2 from MGDG (23.0-35.5 ppm) or SQDG (22.7-34.6 ppm) [6]
25.0	68	24.7	27	FA chain C3 (25.0 ppm) [1], PC C3$\alpha\beta$ (24.7-24.8 ppm) [3]; CH_2 from MGDG (23.0-35.5 ppm) or SQDG (22.7-34.6 ppm) [6]
22.7	52	22.7	78	FA chain C*H_2-CH_3 (22.5-22.6 ppm) [3,5], (22.6-22.8 ppm) [1]; CH_2 from MGDG (23.0-35.5 ppm) or SQDG CH2 (22.7-34.6 ppm) [6]
21.0	18	20.6	43	FA chain CH_2 (20.3 ppm) [5], (20.6 ppm) [1]
		19.5	7	
18.9	37	18.8	11	
15.6	34	16.4	50	
14.2	14	14.1	64	FA terminal CH_3: for DHA (14.0 ppm) [5]; (13.8-14.0 ppm) [3]; MGDG and SQDG (14.4 ppm) [6]; PC (14.5 ppm)[2]; EPA (13.8-14.5 ppm) [4]
12.9	14			
		8.3	6	

Table S3: ^{13}C chemical shifts and relative intensity of lipids peaks obtained for *Chlamydomonas reinhardtii* by cross-polarization (rigid) or RINEPT (mobile). Assignments according to literature values.

Rigid zones (CP)		Mobile zones (RINEPT)		Literature values
δ (ppm)	%	δ (ppm)	%	
174.7	20			DGTS C1 (174.7 ppm) [11]
		131.4	12	C=C from DHA C20 (131.3 ppm) [5]
129.7	12	129.4	24	C=C from: DGTS (129.9 ppm) [11]; glyceryl trioleate (129.5 ppm) [3]; 16:1 C9 or C10; EPA C5 or C6 (129.6-130.1 ppm) [1];
128.0	11	128.1	37	C=C from: FA (127.4-128.4 ppm) [1,5], FA (127.8-127.9 ppm) [3], EPA C11, C14 (127.6-127.9 ppm) [1], MGDG (127 ppm) [6], EPA (127.1-129.2 ppm) [4]
		124.0	12	
		123.0	11	
115.2	8	115.6	14	
103.6	6	103.1	14	MGDG G1 (103.4 ppm) [6], (104 ppm) [7]
		100.5	17	
99.1	13			SQDG G1 (99.4 ppm) [6]
		97.3	12	
81.8	9			
		80.3	9	
		78.1	15	
		76.9	21	
		75.5	20	SQDG G4 (75.3 ppm) [6]
73.3	31	73.1	25	MGDG G2 (72.9 ppm) [6]; SQDG G2 (73.1 ppm) or G3 (73.0 ppm) [6]
		71.9	30	MGDG G3 (72 ppm) [7]
		71.0	21	MGDG G2 (71 ppm), G3 (71.1 ppm) [6]
70.3	17			Glyc C2 (69.9 ppm) [6]; MGDG Gly C2 (69.9 ppm) [6] (70 ppm) [7]; DGTS Glyc C3 (70.5 ppm) [11]
		69.4	24	MGDG G4 (68.8 ppm) or SQDG G5 (69.7 ppm) [6];
65.1	21	67.3	17	MGDG Glyc C1 (67.7 ppm) [6]
		62.9	27	PC Glyc C1 (62.8 ppm) [5]; MGDG Glyc C3 (63 ppm) [7]
		61.5	73	Glyc C1, C3 (61.7-62.0) ppm) [1,3]; Hyp-O-glycan C2 (61.7-61.9 ppm) [12]
60.9	46	60.5	37	PC Cα (60.3 ppm) [2]; MGDG G6 (60 ppm) [7]; Hyp-O-glycan C2 (61.1 ppm) [12]
		58.9	42	
		57.6	21	
54.3	55	53.9	12	Betaine $(CH_3)_3$ (54 ppm) [10]; PC Cγ (54.0 ppm) [5]
		52.1	62	Hyp-O-glycan C5 (52.3-52.9 ppm) [12]
		50.0	11	
48.2	8	48.1	10	
39.3	49	39.8	28	
		37.6	14	Hyp-O-glycan C3 (37.1-37.8 ppm) [12]
		33.8	12	FA chain CH_2 from: PC C12 (33.8 ppm)[2]; C2α,β (33.5-33.9 ppm)[3], (33.8-34.0 ppm) [1,5]; EPA C2 (33.4 ppm) [1]; MGDG (23.0-35.5 ppm) or SQDG (22.7-34.6 ppm) [6]; EPA (26.4-33.5 ppm) [4]
32.4	91	32.2	24	FA chain CH_2 from: n-9 on saturated FAs (32.1-32.2 ppm) [1]; MGDG (23.0-35.5 ppm) or SQDG (22.7-34.6 ppm) [6]
29.8	100	29.8	50	FA chain (CH_2)n (29.3-30.1 ppm) [1,3,5],; EPA (26.4-33.5 ppm) [4]; MGDG (23.0-35.5 ppm) or SQDG (22.7-34.6 ppm) [6]
27.2	57	27.2	34	FA chain allylic CH_2 (-C-C=) (27.1 ppm) [3], (27.3-27.4 ppm) [1]; from EPA

				(26.4-33.5 ppm) [4]; CH_2 from MGDG (23.0-35.5 ppm) or SQDG (22.7-34.6 ppm) [6]
		25.5	30	FA chain allyl (=C-C-C=) (25.4-25.6 ppm) [1,3]; CH_2 from MGDG (23.0-35.5 ppm) or SQDG (22.7-34.6 ppm) [6]
24.8	72	25.0	30	FA chain C3 (25.0 ppm) [1], PC C3$\alpha\beta$ (24.7-24.8 ppm) [3]; CH_2 from MGDG (23.0-35.5 ppm) or SQDG (22.7-34.6 ppm) [6]
22.5	44	22.7	50	FA chain C*H_2-CH_3 (22.5-22.6 ppm) [3,5], (22.6-22.8 ppm) [1]; CH_2 from MGDG (23.0-35.5 ppm) or SQDG CH2 (22.7-34.6 ppm) [6]
20.6	61	20.5	29	FA chain CH_2 (20.3 ppm) [5], (20.6 ppm) [1]
19.3	34	19.6	18	
		17.5	17	
		16.8	20	
		16.2	16	
14.8	30	14.2	100	FA terminal CH_3: for DHA (14.0 ppm) [5]; (13.8-14.0 ppm) [3]; MGDG and SQDG (14.4 ppm) [6]; PC (14.5 ppm)[2]; EPA (13.8-14.5 ppm) [4]; DGTS (14.7 ppm) [11]

References:

[1] M.S. Chauton, T.R. Størseth, J. Krane, High-resolution magic angle spinning NMR analysis of whole cells of *Chaetoceros muelleri* (Bacillariophyceae) and comparison with ^{13}C-NMR and distortionless enhancement by polarization transfer ^{13}C-NMR analysis of lipophilic extracts, J. Phycol., 40 (2004) 611-618.

[2] M. Bouchard, C. Le Guernevé, M. Auger, Comparison between the dynamics of lipid/gramicidin A systems in the lamellar and hexagonal phases: a solid-state ^{13}C NMR study, Biochim. Biophys. Acta, 1415 (1998) 181-192.

[3] C.M. Beal, M.E. Webber, R.S. Ruoff, R.E. Hebner, Lipid analysis of *Neochloris oleoabundans* by liquid state NMR, Biotechnol. Bioeng., 106 (2010) 573-583.

[4] F.D. Gunstone, ^{13}C-NMR spectroscopy of fatty acids and derivatives - Polyunsaturated Fatty Acids, AOCS Lipid Library, 2007, April 10, 2014.

[5] S. Everts, J.H. Davis, ^{1}H and ^{13}C NMR of multilamellar dispersions of polyunsaturated (22:6) phospholipids, Biophys. J., 79 885-897.

[6] L.M. de Souza, M. Iacomini, P.A.J. Gorin, R.S. Sari, M.A. Haddad, G.L. Sassaki, Glyco- and sphingophosphonolipids from the medusa *Phyllorhiza punctata*: NMR and ESI-MS/MS fingerprints, Chem. Phys. Lipids, 145 (2007) 85-96.

[7] V. Castro, S.V. Dvinskikh, G. Widmalm, D. Sandström, A. Maliniak, NMR studies of membranes composed of glycolipids and phospholipids, Biochim. Biophys. Acta, 1768 (2007) 2432-2437.

[8] A.P. Sobolev, E. Brosio, R. Gianferri, A.L. Segre, Metabolic profile of lettuce leaves by high-field NMR spectra, Magn. Reson. Chem., 43 (2005) 625-638.

[9] Human metabolome database, Betaine, The Metabolics Innovation Center, April 10, 2014.

[10] N. Sato, Betaine lipids, Bot. Mag. Tokyo, 105 (1992) 185-197.

[11] A. Banskota, R. Stefanova, S. Sperker, P. McGinn, New diacylglyceryltrimethylhomoserines from the marine microalga *Nannochloropsis granulata* and their nitric oxide inhibitory activity, J. Appl. Phycol., 25 (2013) 1513-1521.

[12] K. Bollig, M. Lamshöft, K. Schweimer, F.-J. Marner, H. Budzikiewicz, S. Waffenschmidt, Structural analysis of linear hydroxyproline-bound O-glycans of *Chlamydomonas reinhardtii*—conservation of the inner core in *Chlamydomonas* and land plants, Carbohyd. Res., 342 (2007) 2557-2566.